SEBS MODULE BEAM: A PRACTICAL TOOL FOR SURFACE ENERGY BALANCE ESTIMATES FROM REMOTE SENSING DATA

Wang L.(1), Parodi G. N.(1), Su Z.(1)

(1) International Institute for Geo-Information Science and Earth Observation – ITC. WRS. P.O.Box 6, 7500 AA Enschede, The Netherlands, Email: lichun@itc.nl

1 ABSTRACT

The SEBS algorithm [1] is an extension of the SEBI concept with a dynamic model for thermal roughness [2], the Bulk Atmospheric Similarity (BAS) theory [3] for PBL scaling and the Monin-Obukhov Atmospheric Surface Layer (ASL) similarity for surface layer scaling. SEBS can be used for local and regional scaling under all atmospheric stability regimes thus providing a link for radiometric measurements and atmospheric models. SEBS is implemented as a "BEAM" module for ATSR [10]. ATSR imagery is radiometrically calibrated and atmospherically for the pre-processing. Meteorological information and radiatives maps complete the input dataset. SEBS results in maps of Rn, LE, H, G, H_{wet} and H_{dry} limit, evaporative fraction, AET instantaneous and daily, and complementary files as standard outputs.

2 BACKGROUND

SEBS consists of a set of tools for the determination of the land surface physical properties and state variables, such as albedo, emissivity, temperature, vegetation coverage etc. from spectral reflectance and radiance; an extended model for the determination of the roughness length for heat transfer [2]; and a new formulation for the determination of the evaporative fraction from the energy balance at limiting cases.

SEBS requires as inputs three sets of information. The first set are land surface properties derived from RS and some additional ground data (albedo, emissivity, temperature, fractional vegetation, LAI, and the height of the vegetation or roughness height, where NDVI could be used as a surrogate). The second set is related to meteorological data or maps of air pressure, air temperature, humidity, and wind speed at a reference height (PBL or ASL). This data can also consist of estimates by a large scale meteorological model. The third data set deals with incoming SW and LW radiation either from direct measurements, model output or parameterization.

SEBS was validated under a wide range of environmental and climatological conditions; it was tested versus AET rates in a semiarid inland basin in NW China [4];[5], and for drought disaster monitoring [6]. It evaluated well as compared with other remote sensing techniques over irrigated fields [7]; [8]; [9]; [2], [5].

This paper will emphasize the requirements, main equations and procedures considered in the present version of software tool. The theory is fully explained in [2].

3 DISTINCTIVE ASPECTS OF SEBS

SEBS for BEAM is a single source model, having some similar and distinctive characteristics compared to their predecessors SEBI [11], SEBAL [12] and S-SEBI [13].

- The latent heat flux is calculated from the evaporative fraction (that is assumed conservative in the day) and the available energy for the process.
- The evaporative fraction is constructed as the sensible heat flux partition from two limiting cases, the dry limit and the wet limit as in SEBI. The quantification of these two constrains is consistent. It does not depend on judgements or subjective/supervised selections. The software shows graphical limits on request (see Figure 1).
- The radiation balance, the limiting cases and the evaporative fraction are calculated on pixel basis. In this way, input maps are matrix of information with spatial independence reducing the calculation time.
- The roughness length for heat transfer is not a constant portion of the roughness length for momentum, but is calculated on pixel basis as a model extended by [2] from the work of [14] and [15] for vegetation canopy, and [16] for bare soil. A new equation term describes the vegetation-bare soil interaction. The theoretical concepts leading to the evolution of this model are explained in [17].
- For that, SEBS has in-built two models for the estimation of the stability parameters needed for the sensible heat. If the reference height (i.e. height of the measurements) is below the top of the Atmospheric Surface Layer (ASL) then Monin-Obukov Similarity (MOS) functions are invoked. If measurements are taken in the outer ASL, then the Bulk Atmospheric Similarity model [3] is used. For measurements at the ground, MOS set is used, but SEBS is prepared to use measurements/outputs of atmospheric models to estimate fluxes when plugged in the BAS. The criterion of using MOS or BAS is evaluated automatically by SEBS using a simplified decision rule based on [3] and described in [18].

Proc. of the '2nd MERIS / (A)ATSR User Workshop', Frascati, Italy 22–26 September 2008 (ESA SP-666, November 2008)

4 SEBS FOR BEAM STRUCTURE

In the following section a description of the input data, pre-processing, parameter model builders selected for SEBS, SEBS-core routines and output will be briefly described.
Figure 1 shows the three main set of procedures for SEBS.
The INPUT is the one requiring most of the effort from the user since sensibility analysis done for SEBS indicates that meteorological and roughness data produces most of the error in the results. This observation can be extended to any available SEB model.
The CORE is the SEBS calculations without user interaction. As such the main methods will be described for user information only. Customization of these methods is a plausible alternative for every situation that the authors are willing to consider.
The OUTPUTS are standard raster thematic maps of fluxes and complementary properties and parameters that could be exported to any other desirable format.

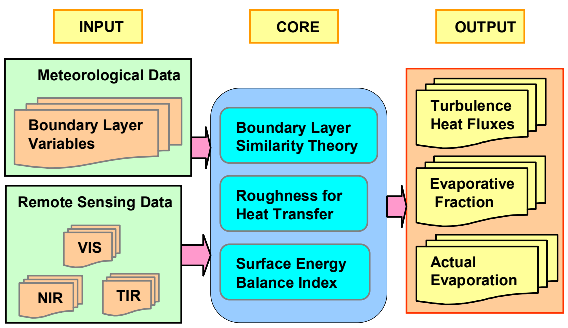

Figure 1: Components of the SEBS for BEAM software.

5 INPUT FOR SEBS ATSR

SEBS as module of BEAM, uses a BEAM-DIMAP, data format (see on-line BEAM manual).
The SEBS Processor uses ATSR "thermal" bands T_{12} and T_{11}, and atmospherically corrected "visible" bands $\rho_{0.87}$ (IR) and $\rho_{0.67}$ (Red) as spatial input. This simple processor does not take any flags into account; it just performs the calculation over the whole product.
Meteorological input is assumed constant for this first version of SEBS for BEAM. Spatial distribution of this input is possible as BEAM capabilities to handle external maps increase.

5.1. Pre-processing of the Spatial Input

If visible atmospherically corrected ATSR images are available they are used as direct input in SEBS4BEAM. The alternative is to use the SMAC4BEAM processor.
The original SMAC algorithm [19] was adapted for ATSR. It requires input on aerosol optical depth (550 µm) or horizontal visibility [km], average air pressure [hPa], ozone content [cm.atm] and water vapour content [g/cm^2] all assumed constant over the image. The definition of the aerosol model available is either continental or desertic. SMAC runs only once and multiple visible band outputs are treated simultaneously. The outputs of SMAC are atmospherically corrected visible bands that will be used as input for SEBS.
After atmospheric correction the SEBS module is ready to operate.

5.2. Meteorological input

Meteorological input is entered in the I/O Parameters tab of the SEBS Processor interface.
A detail on the meteorological information required is:

- Reference height (z_{ref}): height from the ground where measurements of temperature, wind, pressure and specific humidity are made [m].
- Specific Humidity: [kg.kg^{-1}].
- Wind speed (u_{ref}): [m.s^{-1}].
- Air Temperature at reference height (T_a): [°C].
- Air Pressure at reference height: [Pa].
- Air Pressure at land surface: [Pa].
- PBL height (h_i): Height of the Planetary Boundary Layer (PBL) in [m] that can be estimated by radiosounding or using atmospheric model outputs [17]. By default h_i=1000 m.
- Solar radiation: an areal constant downward shortwave radiation in [Watt/m^2] is input in this version. This version supports the estimation of the solar radiation from the visibility and information of the header files, although a direct measurement is always desirable.

All meteorological input must be instantaneous information collected at the time of "satellite pass".

5.3. Optional Input

Two desirable input files that are optional in SEBS.

1) The Landuse file contains classes associated with vegetation height values.
2) The Leaf Area Index file. This input should be in a map named "leaf_area_index". Otherwise, a surrogate calculated value of LAI is used.

These files should be produced in BEAM-DIMAP format for use. Validation tests have demonstrated the importance of these optional inputs to support a better estimation of the aerodynamic roughness height.

5.4. The Landuse Parameter Tab

Aerodynamic roughness, (often displacement height is linked to it), is recognized as the main source of actual evapotranspiration (AET) error in all available "SEB" schematizations since influences greatly the turbulent characteristics near the surface where the heat fluxes originate.
Currently, there are several methods that can be used for its determination (see Table 1).

Table 1: Methods for the estimation of z0m

Method	Input needed
z_{0m} = 0.136 h	Vegetation height map (h)
z_{0m} from LUT. Several	Vegetation map & z_{0m} LUT
z_{0m}= F(VI). Many models	Vegetation index maps
z_{0m} from modelling	Landuse + veg. structure
LIDAR	Experimental. Costly.
Retrievals from wind profiles	Point values

SEBS4BEAM adopts the LUT option from a given Landuse map as main source of z_{0m}.

- In case that the landuse map is known, it is entered as associated to the input file in a new band called "land_use_class" having values between 1 to 25 (depending on landuse). Only in this case, the Landuse parameter TAB becomes active.

In the LUT, all 25 landuse classes have a vegetation height (h) assigned by default. 'z_{0m}' for these classes are calculated as 0.136*h also as default. The user has the option to modify the defaults 'h' and 'z_{0m}' by operating 2 check-boxes as indicated in Table 2.
These classes relate to the PELCOM landuse database [20] that will be used for the estimation of the roughness height from a LUT.

Table 2: Options for z0m estimation (landuse is known).

Check boxes		Options	h [m]	z_{0m} [m]
z_{0m} =0.136*h	z_{0m} = default			
checked	Not checked	Default	default	$0.136*h_{default}$
checked	Not checked	1	user	0.136*h
Not checked	Not checked	2	user	user
Not checked	checked	3	user	$0.136*h_{default}$

- If the landuse map is unknown, the landuse parameter TAB becomes inactive. In this case it is assumed that the vegetation distribution is unknown.

The adopted simplified solution in SEBS is valid only for low vegetation. First, the estimation of the vegetation height (assigning a max. of 0.8 m and a min. of 0 m) weighted by the NDVI. Then the previously default 'z_{0m}' equation is used.

6 SEBS DATA PROCESSING

In this section a brief description of the SEBS "calculation flow" routines to ultimately estimate latent heat flux is explained. Moreover, models for the estimations of intermediate parameters are also explained to allow evaluation of the software applicability regarding the available input.
The energy balance equation in its instantaneous form is expressed as:

$$R_n = G_0 + H + \lambda E \qquad (1)$$

Where: R_n is the net radiation, G_0 is the soil heat flux, H is the turbulent sensible heat flux, and λE is the turbulent latent heat flux (λ is the latent heat of vaporization) and E is the actual evapotranspiration obtained as residual of this equation. All units in [watt m^{-2}].

6.1. Net Radiation

$$R_n = (1-\alpha)\cdot R_{swd} + \varepsilon \cdot R_{lwd} - \varepsilon \cdot \sigma \cdot T_0^4 \qquad (2)$$

Where: α is the albedo [-], R_{swd} [watt m^{-2}] is the downward solar radiation, R_{lwd} [watt m^{-2}] is the downward longwave radiation, ε [-] is the emissivity of the surface, σ [watt m^{-2} K^{-4}] is the Stefan-Bolzmann constant, and T_0 [K] is the surface temperature.

The choices for R_{swd} are: direct input by the user as a single value for the entire image (desirable), or an estimation from:

$$R_{swd} = I_{sc} \cdot e_0 \cdot \cos\theta_z \cdot \exp(-m \cdot \tau) \qquad (3)$$

where I_{sc}= 1367 watt.m^{-2}, is the solar constant, e_0 the eccentricity factor, θ_z the solar zenith angle stored in the N1 format, 'm' the air mass, and 'τ' the optical thickness.
The horizontal visibility is used to estimate the extinction coefficient following [21].
R_{lwd} is calculated from $R_{lwd} = \varepsilon_a \sigma T_a^4$ where ε_a is the apparent emissivity of the atmosphere calculated as $\varepsilon_a = 9.2 \cdot 10^{-6} \cdot (T_a + 273.15)^2$ and T_a is the air temperature at the reference height (input).
Broadband albedo is taken from the visible channels following [22].
The surface temperature 'T_0' is evaluated from the thermal vertical ATSR channel 1 and 2 (12 and 11 µm and the content of water vapour 'W'. The selected algorithm was performing the best after the EAGLE campaign in Barrax, 2003.

$$\begin{aligned} T_0 &= T_{2n} + (1.97 + 0.2W)\cdot(T_{2n} - T_{1n}) - \\ &(0.26 - 0.08W)\cdot(T_{2n} - T_{1n})^2 + (0.02 - 0.67W) \\ &+ (64.5 - 7.35W)\cdot(1-\varepsilon) - (119 - 20.4W)\cdot\Delta\varepsilon \end{aligned} \qquad (4)$$

If no other information 'W' is taken from [23]. The evaluation of the emissivity follows [24] adapted to ATSR [25].
Here, $\bar{\varepsilon} = (\varepsilon_{11} + \varepsilon_{12})/2$ and $\Delta\varepsilon = \varepsilon_{12} - \varepsilon_{11}$
NDVI is calculated first from atmospherically corrected $\rho_{0.87}$ (IR) and $\rho_{0.67}$ (Red).
If 0.2<NDVI then the pixel is considered bare.
In this case:

$$\begin{aligned} \bar{\varepsilon} &= 0.9825 - 0.051 \cdot \rho_{0.67} \ and \\ \Delta\varepsilon &= -0.0001 - 0.0041 \cdot \rho_{0.67} \end{aligned} \qquad (5)$$

If NDVI>0.5 then the pixel is considered full cover. In this case $\bar{\varepsilon} = 0.99$ *and* $\Delta\varepsilon = 0$.
For mixed pixels (0.2<NDVI<0.5)

$$P_v = \left(\frac{NDVI - NDVI_{min}}{NDVI_{max} - NDVI_{min}} \right)^2 \quad (6)$$

$$\bar{\varepsilon} = 0.971 + 0.018 \cdot P_v \ \ and \ \ \Delta\varepsilon = 0.006 \cdot (1 - P_v) \quad (7)$$

Water bodies should be filtered from this classification and the emissivity should be reassigned (default: 0.995). In SEBS this assignation is done to all pixels having surface broadband albedo < 0.035.

6.2. Soil Heat Flux

In SEBS, the soil heat flux is estimated as: $G_0 = R_n \cdot [\Gamma_c + (1 - P_v) \cdot (\Gamma_s - \Gamma_c)]$ where 'Γ_c' and Γ_s' are the proportions of G_0/R_n for full cover and bare soil, fixed as 0.05 and 0.315 respectively. The fractional vegetation cover 'P_v' weights between limiting cases.

6.3. SEBS core processing

Until here all direct, surrogate and modeled input to SEBS4BEAM was explained. Customization of input routines could eventually be done by readapting the methods that fit better the available information if required. This section explains the SEBS core routines [1] that calculate the SEBS outputs without interaction with the user.

6.3.1. Establishing MOS or BAS equation set

SEBS contains a set of rules to plug either MOS or BAS theory in the estimation of H.

In SEBS the top of the PBL height (h_i) is input data. The height of the ASL (h_{st}) is found proportional to h_i [3] over moderated rough terrain and proportional to the surface roughness over very rough terrain.

Then SEBS adopts h_{st} equal to the largest between:

$h_{st} = \alpha_b \cdot h_i$ [$0.10 \le \alpha_b \le 0.15$; 0.12 default in SEBS] or $h_{st} = \beta_b \cdot z_{0m}$ [$100 \le \beta_b \le 150$; 125 default in SEBS]. Then z_{0m}= 0.96 m separates moderate rough from very rough terrain if 'h_i' is assumed equal to 1000 m.

If the reference height (z_{ref}) is lower than h_{st}, then MOS set of equation applies, otherwise BAS does. The use of BAS equations is limited to data input obtained from high altitudes, what makes SEBS4BEAM adequate for atmospheric model coupling.

6.3.2. The roughness length for heat transfer z_{oh}

In SEBS, $z_{0h} = z_{0m} / \exp(kB^{-1})$. To estimate the kB^{-1} value, an extended model of [2] is proposed as follows:

$$kB^{-1} = \frac{kC_d}{4C_t \frac{u_*}{u(h)}\left(1 - e^{-n_{ec}/2}\right)} f_c^2 + \ldots$$
$$\ldots + 2 f_c f_s \frac{k \cdot {}^{u_*}\!/_{u(h)} \cdot {}^{z_{0m}}\!/_h}{C_t^*} + kB_s^{-1} f_s^2 \quad (8)$$

where $f_c = P_v$ is the fractional canopy coverage and f_s is its complement. C_t is the heat transfer coefficient of the leaf. For most canopies and environmental conditions, $0.005.N \le C_t \le 0.075.N$ (N is number of sides of a leaf participating in the heat exchange), The heat transfer coefficient of the soil is given by $C_t^* = Pr^{-2/3}.Re_*^{-1/2}$, where 'Pr' is the Prandtl number, the roughness Reynolds number $Re_* = h_s.u_*/\nu$, with h_s the roughness height of the soil and u_* the friction velocity.

'N_{ec}' is the within-canopy wind speed profile extinction coefficient [14], the kinematic viscosity of the air is given by $\nu = 1.327.10^{-5}.(p_0/p).(T_a/T_{a0})^{1.81}$ [14], with p and T_a the ambient pressure and temperature and p_0=101.3 kPa and T_{a0} =273.15 K. Physically and geometrically, the first term of (8) follows the full canopy (only) model of [15], the third term is that of [16] for a bare soil surface, while the second term describes the interaction between vegetation and bare soil surface. A quadratic weighting based on the fractional canopy coverage is used to accommodate any situation between the full vegetation and bare soil conditions. For bare soil surface kB_s^{-1} is calculated according to [16]:

$$kB_s^{-1} = 2.46(\mathrm{Re}_*)^{1/4} - \ln[7.4] \quad (9)$$

The following parameterization makes possible the estimation of kB^{-1} from z_{om}, h, $u(z_{ref})$, f_c, T_a and p:

$$LAI = [NDVI \cdot (1 + NDVI)/(1 - NDVI)]^{0.5} \quad (10)$$

for low vegetation only [26];

$u_*/u(h) = 0.32 - 0.264 \cdot e^{-15.1 \cdot C_d \cdot LAI}$; C_t= 0.01; C_d= $0.2{*}C_t$; h (vegetation height)= $z_{om}/0.136$; d_0 (zero plane displacement) = 0.667.h;

$$n_{ec} = C_d \cdot LAI / \left[2 \cdot (u_*/u(h))^2\right] \quad (11)$$

$$u(h) = u(z_{ref}) \cdot \ln((h - d_0)/z_{0m}) / \ln((z_{ref} - d_0)/z_{0m}) \quad (12)$$

$$u_* = u(z_{ref}) \cdot k / \ln[(z_{ref} - d_0)/z_{0m}] \quad (13)$$

calculated at measuring point;

$$\mathrm{Re}_* = (u_*/u(h)) \cdot u(h) \cdot (h/\nu) \quad (14)$$

$$C_t^* = \mathrm{Pr}^{-2/3} \cdot \mathrm{Re}^{-1/2} = 0.7 \cdot h_s \cdot u_*^{soil} / \nu \quad (15)$$

$$u_*^{Soil} = u(z_{ref}) \cdot k / (\ln(z_{ref}/h_{soil})) \quad (16)$$

Where the roughness height for soil h_{soil} is adopted equal to 0.009 m; and $Re_* = h_s \cdot u_*^{Soil} / \nu$.

6.3.3. Sensible heat flux 'H' at limiting cases, H_{dry} and H_{wet}

If MOS applies the set of equations established in an iterative scheme to evaluate H is:

$$u = \frac{u_*}{k}\left[\ln\left(\frac{z-d_0}{z_{0m}}\right) - \Psi_m\left(\frac{z-d_0}{L}\right) + \Psi_m\left(\frac{z_{0m}}{L}\right)\right] \quad (17)$$

$$\theta_0 - \theta_a = \frac{H}{ku_*\rho C_p}\left[\ln\left(\frac{z-d_0}{z_{0h}}\right) - \Psi_h\left(\frac{z-d_0}{L}\right) + \Psi_h\left(\frac{z_{0h}}{L}\right)\right] \quad (18)$$

$$L = -\frac{\rho \cdot C_p \cdot u_*^3 \cdot \theta_v}{k \cdot g \cdot H} \quad (19)$$

θ_0 and θ_a are the potential surface and air (at reference height) temperature respectively and θ_v is the mean virtual potential temperature. The stability correction functions for stable atmosphere are defined by [3] as:

$$\begin{cases} \Psi_m(y) = \ln(a+y) - 3 \cdot b \cdot y^{1/3} + \frac{b \cdot a^{1/3}}{2}\ln\left[\frac{(1+x)^2}{(1-x+x^2)}\right] + .. \\ .. + 3^{1/2} \cdot b \cdot a^{1/3}\tan^{-1}\left[\frac{(2 \cdot x - 1)}{3^{1/2}}\right] + \Psi_0, \quad for \quad y \le b^{-3} \\ \Psi_m(y) = \Psi_m(b^{-3}), \quad for \quad y > b^{-3} \end{cases} \quad (20)$$

$$\Psi_h(y) = [(1-d_0)/n] \cdot \ln[(c+y^n)/c] \quad (21)$$

$$y = -(z-d)/L; \; x = (y/a)^{1/3} \; and \quad \Psi_0 = \left(-\ln a + 3^{1/2} \cdot b \cdot a^{1/3} \cdot \pi/6\right) \quad (22)$$

[3] evaluated these values from databases provided by [27], and [28]: a= 0.33; b= 0.41; m= 1.0; c=0.33; d=0.057 and n= 0.78.

If unstable atmosphere applies, then the set of functions developed by [29] and evaluated by [30] are used.

$$\Psi_m = -\left[a_s \cdot y_s + b_s\left(y_s - \frac{c_s}{d_s}\right)\exp(-d_s \cdot y_s) + b_s\frac{c_s}{d_s}\right] \quad (23)$$

$$\Psi_h = -\left[\left(1 + \frac{2a_s}{3}y_s\right)^{1.5} + b_s\left(y_s - \frac{c_s}{d_s}\right)\exp(-d_s \cdot y_s) + \left(\frac{b_s \cdot c_s}{d_s} - 1\right)\right] \quad (24)$$

where: $y_s = (z-d)/L$, a_s= 1; b_s=2/3; c_s= 5 and d_s= 1.

In all these parameterization: z is the height above the surface (normally coincides with z_{ref}), $u_* = (\tau_0/\rho)^{0.5}$ is the friction velocity, τ_0 is the surface shear stress, ρ is the density of air, k=0.41 is the von Karman constant, Ψ_m and Ψ_h are the stability correction functions for momentum and sensible heat transfer respectively, L is the Obukhov length.

If BAS applies, then the set of equations used for the calculation of H is a function of the terrain roughness.

$$u_*/u_{mix} = k \cdot [\ln(h_i/z_{0m}) - B_w \cdot (-h_i/L)]^{-1} \quad (25)$$

$$H/[u_* \cdot (\theta_0 - \theta_{mix})] = k \cdot [\ln(h_i/z_{0h}) - C_w \cdot (-h_i/L)]^{-1} \quad (26)$$

For unstable cases:
For moderately rough terrain { $z_{0m} < (\alpha_b/\beta_b) \cdot h_i$ }

$$B_w = -\ln(\alpha_b) + \Psi_m(\alpha_b \cdot h_i/L) - \Psi_m(z_{0m}/L) \quad (27)$$

$$C_w = -\ln(\alpha_b) + \Psi_h(\alpha_b \cdot h_i/L) - \Psi_h(z_{0h}/L) \quad (28)$$

For very rough terrain { $z_{0m} \ge (\alpha_b/\beta_b) \cdot h_i$ }

$$B_w = -\ln(h_i/(\beta_b z_{0m})) + \Psi_m(\beta_b z_{0m}/L) - \Psi_m(z_{0m}/L) \quad (29)$$

$$C_w = -\ln(h_i/(\beta_b z_{0m})) + \Psi_h(\beta_b z_{0m}/L) - \Psi_h(z_{0h}/L) \quad (30)$$

For stable cases:

$$B_w = -2.2 \cdot \ln(1 + h_i/L) \; and \quad C_w = -7.6 \cdot \ln(1 + h_i/L) \quad (31)$$

Where 'mix' subscript indicates average of the variable in question over the lower half of the mixed layer.

The friction velocity, the sensible heat flux and the Obukhov stability length are obtained in SEBS solving the system of non-linear equations as explained later. It is important to note that the derivation of the sensible heat flux requires only the wind speed and temperature at the reference height as well as the surface temperature and is independent of other surface energy balance terms.

In order to determine the evaporative fraction, use is made of energy balance considerations at limiting cases. Then, this derived 'H' is further subjected to constraints in the range set by the sensible heat flux at the wet limit H_{wet}, and at dry limit H_{dry} in SEBS.

Under the assumption of dry-limit, the $\lambda E \rightarrow 0$ due to restricted soil moisture and the sensible heat flux is at its maximum value. Then H_{dry} is calculated as:

$$\lambda E_{dry} = R_n - G_0 - H_{dry} \equiv 0, \quad H_{dry} = R_n - G_0 \quad (32)$$

At the wet limit, λE_{wet} reaches a maximum and H_{dry} a minimum, but not zero. At the same time, λE_{wet} coincides with potential evapotranspiration and its value could be derived from a Penman-Monteith type of equation (after [31])

$$\lambda E = \frac{\Delta \cdot r_e \cdot (R_n - G_0) + \rho C_p \cdot (e_{sat} - e)}{r_e \cdot (\gamma + \Delta) + \gamma \cdot r_i} \quad (33)$$

where 'e' and 'e_{sat}' are actual and saturation vapour pressure respectively; 'γ' is the psychrometric constant, and Δ is the rate of change of saturation vapour pressure with temperature; 'r_i' is the bulk surface internal resistance (stomata) and 'r_e' is the external or aerodynamic resistance. At the wet-limit, the internal resistance $r_i \equiv 0$ by definition, then H_{wet} is evaluated as:

$$H_{wet} = \left((R_n - G_0) - \frac{\rho C_p}{r_{ew}} \cdot \frac{e_s - e}{\gamma} \right) \Big/ \left(1 + \frac{\Delta}{\gamma} \right) \quad (34)$$

Since the external resistance r_e depends on 'L', the external resistance at wet limit is expressed as:

$$r_{ew} = \frac{1}{ku_*} \left[\ln\left(\frac{z - d_0}{z_{0h}}\right) - \Psi_h\left(\frac{z - d_0}{L_w}\right) + \Psi_h\left(\frac{z_{0h}}{L_w}\right) \right] \quad (35)$$

Where L_w can be calculated as:

$$L_w = -\frac{\rho u_*^3}{kg \cdot 0.61 \cdot (R_n - G_0)/\lambda} \quad (36)$$

Figure 2 illustrates the use of wet and dry limits in SEBS. For each pixel a value of H, H_{dry} and H_{wet} can be calculated. These two state variables can be expressed as a function of the difference between surface and air temperatures.
The proportions of these temperature differences with respect to the limits are the basis for the estimation of the evaporative fractions.

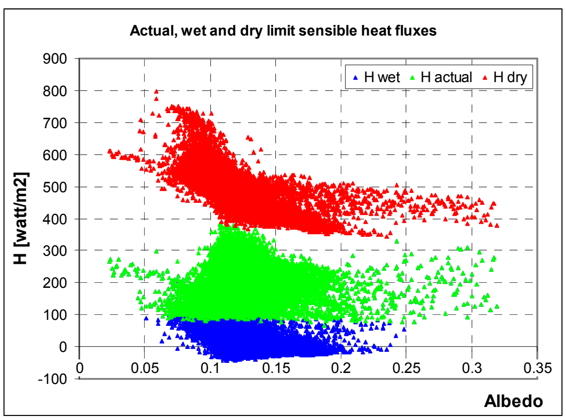

Figure 2: Distribution of wet and dry limits and actual sensible heat flux for an MODIS image obtained along the Qinghan-Tibetan highway in China (12 June 2007 / UTC 04:55). This dataset is part of the research effort to validate the algorithm.

6.4. Iteration sequence

The iteration scheme proposed by SEBS to estimate H is summarized.

1. A first value of H and u* (u_{ini}* and H_{ini}) are initialized assuming neutral stability (all $\Psi_{m/h}$=0), from eqs. (17) to (19).
2. The use of MOS or BAS equations is decided after the reference height is compared to the height of the ASL layer as mentioned earlier, but the iteration procedure is similar for both cases.
3. The iteration sequence calculates:
   a. 'L' from u_{ini}* and H_{ini} from (19)
   b. A new value of u* from (17) or (25)
   c. A new value of H from (18) or (26)

SEBS is set to stop when H_i-H_{i-1} <0.01 or after 100 iterations.

6.5. Heat fluxes and actual evaporation

The relative evaporation is evaluated after the limiting cases:

$$\Lambda_r = \frac{\lambda E}{\lambda E_{wet}} = 1 - \frac{\lambda E_{wet} - \lambda E}{\lambda E_{wet}} = 1 - \frac{H - H_{wet}}{H_{dry} - H_{wet}} \quad (37)$$

Then the evaporative fraction is given as:

$$\Lambda = \frac{\lambda E}{H + \lambda E} = \frac{\lambda E}{R_n - G} = \frac{\Lambda_r \cdot \lambda E_{wet}}{R_n - G} \quad (38)$$

When the average daily net radiation R_n^{day}, soil heat flux (G_0^{day}→0) and evaporative fraction are known, and accepting the indication that the evaporative fraction is conservative [32], [33], [34], the E_{daily} is finally estimated as:

$$E_{daily} = 8.64 \cdot 10^7 \Lambda_0^{24} \frac{\overline{R_n} - \overline{G_0}}{\lambda \cdot \rho_W} = 8.64 \cdot 10^7 \Lambda \frac{\overline{R_n}}{\lambda \cdot \rho_W} \quad (39)$$

$$\overline{R_n} = (1 - \alpha) \cdot K_{24}^{\downarrow} + \varepsilon \cdot L_{24} \quad (40)$$

where $K^{\downarrow}_{24}$ is the daily incoming global radiation and L_{24} is daily net longwave radiation, λ is the latent heat of vaporization (JKg^{-1}), ρ_w is the density of water ($Kg\ m^{-3}$). The daily average albedo, α, and emissivity, ε, can be approximated with the same values as used previously in the energy balance equation.

7 SEBS VALIDATION AND SENSITIVITY ANALYSIS

It is not the purpose of this paper to elaborate on validation analysis, but a reference to the validation efforts is mentioned. SEBS validation was and is currently being done intensively in several research campaigns and trough databases: Cotton dataset [35], the shrub and the grass dataset of [36], Loobos (NL) May 1997, Tormelloso (SP) June 1999. ATSR one-source data was processed in parallel with these two last campaigns in Netherlands and Badajoz, Lleida and Tormelloso (SP). Results are extensively discussed in [18], and it is recommended. Several other efforts were taken in recent years: the EAGLE campaign 2006 where ATSR algorithms were improved and validation with the Cabauw tower was carried out, and several PhD research efforts on the Tibetan Plateau in China.

After reviewing several documents where SEBS validation is addressed, we express here the common concerns on data quality required for better results:

- SEBS appears to show appreciable sensitivity to all input variables, except specific humidity.
- The sensitivity is not constant through the range in which variables are varied; i.e. sensitivity increases dramatically when wind speed or NDVI approaches zero. Using the dataset of [37] it was concluded that the algorithm cannot be used for win speeds lower than 0.5 $m.s^{-1}$.
- In flat areas, air pressure will not cause a large error and a DEM could be used to derive it.
- Air temperature and wind speed are the ground variables most affecting the performance of SEBS.
- It is strongly recommended to obtain information of vegetation height to evaluate the roughness length for momentum minimizing the use of NDVI as surrogate.
- The use of the percentage of vegetation improves the evaluation of roughness length.
- SEBS for BEAM is presently implemented as a single source model. The estimation of evaporation in semiarid to scarcely vegetated areas is better described with the 2-source SEBS, (IDL code) [18].

8 CONCLUSIONS

SEBS4BEAM is a free tool adequate for the estimate of the components of the Energy Balance Equation and overall actual evapotranspiration on daily basis from RS images.

Despite that the algorithm is physically based and intended for any sensor working both in visible and thermal, this application is (as today) restricted to ATSR and MODIS in BEAM due to the specific pre-processing that these sensors require.

The open source nature of the project allows modification and adaptations to specific cases or sensors.

SEBS core is the routine for the evaluation of the sensible heat flux. Different studies have reported that SEBS is sensitive to the meteorological input and the user should carefully evaluate it in order to avoid errors in the estimates of the actual evapotranspiration.

As a single source in this version, SEBS is applicable on semi-dense to dense vegetation cover areas and bare soil areas. More errors are expected from patchy areas of bare soil and mixed vegetation where a two source model might be a better choice.

More sensitivity analysis over SEBS is carried out in the ITC research program, both at PhD and MSc. level in different campaigns in Africa, Asia and Europe where the major concern is better evaluation of the aerodynamic roughness for heat transfer to improve the overall efficiency of the algorithm.

9 REFERENCES

1. Su Z. (2002). The Surface Energy Balance System (Sebs) for Estimation of Turbulent Heat Fluxes. *Hydrology and Earth System Sciences*. **6**, 85-99.
2. Su Z., Schmugge T., Kustas W.P., Massman W.J. (2001). An Evaluation of Two Models for Estimation of the Roughness Height for Heat Transfer between the Land Surface and the Atmosphere. *J. Appl. Meteorol.* **40** (11), 1933-1950.
3. Brutsaert W. (1999). Aspects of Bulk Atmospheric Boundary Layer Similarity under Free-Convective Conditions. *Rev. Geophy.* **37**, 439-451.
4. Li X., (2001). Estimation of Urumqi River Basin Evaporation with Remote Sensing. Hydrology. MSc. Delft, IHE-UNESCO, pp.
5. Su Z., Li X., Zhou Y., Wan L., Wen J., Sintonen K., (2003). *Estimating Areal Evaporation from Remote Sensing*, in International Geoscience And Remote Sensing Symposium Toulouse.
6. Su Z., Yacob A., Wen J., Roerink G., He Y., Gao B., Boogaard H., van Diepen C. (2003). Assessing Relative Soil Moisture with Remote Sensing Data: Theory and Experimental Validation. *Phys. Chem. Earth.* **28** (1-3), 89-101.
7. Norman J., Kustas W.P., Humes K.S. (1995). A Two-Source Approach for Estimating Soil and Vegetation Energy Fluxes in Observations of Directional Surface Temperature. *Agricultural and Forest Meteorology.* **77**, 263-293.
8. Zhan X., Kustas W.P., Humes K.S. (1996). An Intercomparison Study on Models of Sensible Heat Flux over Partial Canopy Surfaces with Remotely Sensed Surface Temperature. *Remote Sens. Environ.* **58**, 242-256.
9. Kustas W.P., Norman J.M. (1999). Evaluation of Soil and Vegetation Heat Flux Predictions Using a Simple Two-Source Model with Radiometric Temperatures for Partial Canopy Cover. *Agric. For. Meteorol.* **94**, 13-29.
10. ESA, (2008). *The Beam Project*. Online at http://www.brockmann-consult.de/beam/downloads.html (as from 4 September 2008).
11. Menenti M., Choudhury B.J., (1993). Parametrization of Land Surface Evapotranspiration Using a Location-Dependent Potential Evapotranspiration and Surface Temperature Range. In *Exchange Processes at the Land Surface for a Range of Space and Time Scales* (Ed. Bolle HJ), IAHS, pp. 561-568.
12. Bastiaanssen W.G.M., (1995). Regionalization of Surface Flux Densities and Moisture Indicators in Composite Terrain – a Remote Sensing Approach under Clear Skies in Mediterranean Climates. Ph.D.

Wageningen, Wageningen Agricultural University, pp. 273.

13. Roerink G.J., Su Z., Menenti M. (2000). S-Sebi: A Simple Remote Sensing Algorithm to Estimate the Surface Energy Balance. *Phys. Chem. Earth.* **25**, 147-157.
14. Massman W.J. (1999). A Model Study of Kb_h^{-1} for Vegetated Surfaces Using 'Localized near-Field' Lagrangian Theory. *J. Hydrol.* **223**, 27-43.
15. Choudhury B.J., Monteith J.L. (1988). A Four Layer Model for the Heat Budget of Homogeneous Land Surfaces. *Q.J.R. Meteorol. Soc.* **114**, 373-398.
16. Brutsaert W., (1982). *Evaporation into the Atmosphere*. D. Reidel, Dordrecht, Holland, pp 287.
17. Su Z., Pelgrum H., Menenti M. (1999). Aggregation Effects of Surface Heterogeneity in Land Surface Processes. *Hydrology and Earth System Sciences.* **3** (4), 549-563.
18. Rauwerda J., Roerink G.J., Su Z., (2002). *Estimation of Evaporative Fractions by the Use of Vegetation and Soil Component Temperatures Determined by Means of Dual-Looking Remote Sensing*. Report num: 580 Wageningen, Alterra, p 147.
19. Rahman H., Dedieu G. (1994). Smac: A Simplified Method for the Atmospheric Correction of Satellite Measurements in the Solar Spectrum. *Int. J. Remote Sensing.* **15** (1), 123-143.
20. Champeaux J.L., Mucher C.A., Steinnocher K., Griguolo S., Wester K., Goutorbe J.P., Kressler F., Heunks C., Van Katwijk V.F., (Year). The Pelcom Project: A 1-Km Pan-European Land Cover Database Forenvironmental Monitoring and Use in Meteorological Models. In *Proc. International Geoscience and Remote Sensing Symposium (IGARSS 2000)*. (Ed. IGARSS.), Honolulu, HI, USA, pp. 1915-1917.
21. Su Z., Wen J., Wan L. (2003). A Methodology for the Retrieval of Land Physical Parameter and Actual Evaporation Using Noaa/Avhrr Data. *Journal of Jilin University.* **33 (sup.)** (Earth Science Edition), 106-118.
22. Valiente J.A., Nunez M., Lopez Baeza E., Moreno J.F. (1995). Narrow-Band to Broad-Band Conversion for Meteosat-Visible Channel and Broad-Band Albedo Using Both Avhrr-1 and -2 Channels. *Int. J. Remote Sensing.* **16** (6), 1147-1166.
23. Li Z.L., Jia L., Su Z., (2001). *Envisat. Land Surface Processes: Estimation of Vegetation and Soil Component Temperatures from Atsr-2 Data*, USP-2 B, (ed). Report num: 1, pp 43-54.
24. Sobrino J.A., Raissouni N. (2000). Toward Remote Sensing Methods for Land Cover Dynamic Monitoring. Application to Morocco. *Int. J. Remote Sensing.* **21** (2), 353-366.
25. Sobrino J., Soria G., (2003). Aatsr Land-Surface Temperature & Emissivity Algorithm Theoretical Basis Document. EAGLE project (SST3-CT-2003-502057), pp. 1-16.
26. Su Z., (1996). Remote Sensing Applied to Hydrology: The Sauer River Basin Study. Hydrologie/Wasserwirtschaft, Faculty of Civil Engineering. Ph.D. Bochum, Germany, Ruhr Univesity, pp.
27. Högström U. (1988). Non-Dimensional Wind and Temperature Profiles in the Atmospheric Surface Layer: A Re-Evaluation. *Boundary-Layer Meteorol.* **42**, 55-78.
28. Kader B.A., Yaglom A.M. (1990). Mean Fields and Fluctuation Moments in Unstable Stratified Bundary Layers. *J. Fluid Mech\.* **212**, 637-662.
29. Beljaars A.C.M., Holtslag A.A.M. (1991). Flux Parameterization over Land Surfaces for Atmospheric Models. *J. Appl. Meteorol.* **30**, 327-341.
30. van den Hurk B.J.J.M., Holtslag A.A.M. (1995). On the Bulk Parameterization of Surface Fluxes for Various Conditions and Parameter Ranges. *Boundary-Layer Meteorol.* **82**, 199-234.
31. Menenti M., (1984). *Physical Aspects of and Determination of Evaporation in Deserts Applying Remote Sensing Techniques.* Report num: 10, Special issue. The Netherlands, Institute for Land and Water Management Research (ICW).
32. Shuttleworth W.J., Gurney R.J., Hsu A.Y., Ormsby J.P. (1989). Fife: The Variation in Energy Partition at Surface Flux Sites. *IAHS Publication.* **186**, 67-74.
33. Sugita M., Brutsaert W. (1991). Daily Evaporation over a Region from Lower Boundary-Layer Profiles Measured with Radiosondes. *Water Resour. Res.* **27** (5), 747-752.
34. Crago R.D. (1996). Comparison of the Evaporative Fraction and the Priestley-Taylor a for Parameterizing Daytime Evaporation. *Water Resour. Res.* **32** (5), 1403-1409.
35. Kustas W.P. (1990). Estimates of Evapotranspiration with a One and Two Layer Model of Heat Transfer over Partial Canopy Layer. *J. Appl. Meteorol.* **29**, 704-715.
36. Kustas W.P., Blanford J.H., Stannard D.I., Daughtry C.S.T., Nichols W.D., Weltz M.A. (1994). Local Energy Flux Estimates for Unstable Conditions Using Variance Data in Semiarid Rangelands. *Water Resour. Res.* **30**, 1351-1361.
37. Kustas W.P., Choudhury B.J., Moran M.S., Reginato R.J., Jackson R.D., Gay L.W., Weaver H.L. (1989). Determination of Sensible Heat Flux over Sparse Canopy Using Thermal Infrared Data. *Agric. For. Meteorol.* **44**, 197-216.